Spring 5-5-2011

Description of Pressure Fluctuations in a Circulating Fluidized Bed by Statistical Analysis

Adam Luckos
Sasol Technology, South Africa, adam.luckos@sasol.com

Roelof Coetzer
Sasol Technology, South Africa

Andre Mostert
Sasol Technology, South Africa

DESCRIPTION OF PRESSURE FLUCTUATIONS IN A CIRCULATING FLUIDIZED BED BY STATISTICAL ANALYSIS

Roelof L.J. Coetzer, Andre Mostert and Adam Luckos
Sasol Technology, Research and Development
1 Klasie Havenga Road, Sasolburg, 1947 South Africa

ABSTRACT

In this paper we evaluate different methods for statistically analyzing the variability in pressure fluctuations measured at three locations in an 80-mm-ID, 5-m-tall CFB model operated with natural rutile particles and air at ambient conditions. The methods evaluated are the Shannon entropy, Fischer information matrix together with kernel density estimation, and an estimation of the magnitude of the pressure amplitudes. The accuracy of the different methods is estimated by the bootstrap method. We illustrate how informative statistics from these methods can be used to quantify the effect of the process variables on fluidization at different bed locations. Depending on the interest of the experimenter, the method and statistic can be selected which explains fluidization operation most accurately.

INTRODUCTION

The continuous monitoring of gas-solid fluidized-bed reactors is an important issue in the industrial practice because of the complex dynamical behaviour characterizing these systems. Failures and difficulties experienced in the operation of fluidized-bed reactors are usually attributed to an un-sufficient understanding of the physics of gas-solid fluidization (1). In particular, our knowledge on systems with irregularly shaped particles with wide size distributions operated at higher gas velocities (in the turbulent regime and in the fast fluidization regime), elevated temperatures and pressures is still relatively poor.

In the last three decades, several techniques have been developed to describe the dynamic phenomena that take place within the bed. Among these techniques, the pressure fluctuation measurements are the most popular owing to their low costs and direct relation to the bed dynamics (2). Pressure measurements sampled at frequencies 20–1000 Hz can be used to describe important fluidized-bed characteristics such as the quality of fluidization, size and frequency of bubbles, transition from bubbling to turbulent regime and minimum fluidization velocity.

In our previous studies, several important process parameters such as critical velocities, distributions of solid concentration and pressure fluctuations were measured in a CFB cold model (3–6). The variability in the pressure fluctuations were previously evaluated by using the standard deviation and the coefficient of variation (7). In this paper, we extend the analysis of the data by applying Shannon entropy and Fisher information matrix (8). Our analysis should establish the relationship between two entities, (1) process variables, and (2) pressure fluctuations at different levels in the riser. This relationship will provide a basis for controlling the operation of a CFB reactor.

TEST APPARATUS AND PROCEDURE

Measurements of pressure fluctuations were carried out in the riser of the 80-mm, 5-m tall CFB cold model made of transparent PVC. Data acquisition units recorded the signals (sampled at 200 Hz) from three pressure transducers located at the bottom (0.2 m above the distributor), in the middle (at 2.46 m), and at the top of the riser (at 4.47 m). All tests were conducted with air at ambient conditions. At each stable condition signals were collected over a period 40 s, an interval producing 8192 (i.e. 2^{13}) pressure readings. The solid material used was natural rutile (TiO_2). Its particles fall into group B of Geldart's classification. They are sub-rounded, fine (80–165 μm) and dense (4085 kg/m^3). A more detailed description of the apparatus and test procedure can be found in an earlier paper on the subject (4).

RESULTS

The concentration of solids in the riser adopts a 'C' shape, which becomes less pronounced as the solid-circulation rate, G_s, at a given superficial fluidizing velocity, U, decreases (4–6). Concomitant with the decrease is a shift in solids concentration at each point in the riser to lower values, and move to greater solids concentrations at the top of the riser than at the bottom. A higher suspension density at the top of the riser—a consequence of the rebounding of particles from the plate closing the top of the riser—is a phenomenon that is well known in small-scale (<0.2 m) CFB units (9–12). In tests at a comparatively low U (3.5 m/s), higher solids concentrations span the top half of the riser (~2.5 m). The suspension density decreases gradually from the top of the riser. At higher fluidizing velocities (U=4.9 and 7.4 m/s) higher solids concentrations are confined to a shorter length of the riser (≤1 m), and the profile is much steeper. As Jin and co-workers showed (13), higher superficial gas velocities increase the velocity of upwardly moving particles, which increases the exchange of momentum between particles moving in opposite directions. As the influence of upwardly moving particles grows stronger (at high gas velocities), the region of momentum exchange shortens. A shortening of the region of higher suspension densities would accompany this change.

Pressures in the riser fluctuate over a range of about 1.2 kPa. The patterns of fluctuations along the length of the riser are similar and synchronized (6). Pressure fluctuations are irregular, and their peak intensities vary. The distribution of pressure at each tap is skewed towards higher values; fluctuations are more pronounced above the mean than below it. Expressing the amplitude of fluctuations over a scanned interval by the standard deviation of pressure readings, one can readily see that (7):

- The average amplitude of pressure fluctuations increases with increasing G_s and *U.*
- The average amplitude of fluctuations is largest at the top of the column; the amplitudes of fluctuations at the middle and bottom of the column are similar—yet the solids concentration is similar at the top and bottom, and different from that in the middle.
- There is an exception to this pattern at high superficial gas velocities. The measurements may be problematic as solids flow bordered on being unstable.

Figure 1 depicts the pressure fluctuations (normalized with respect to the mean pressure) in the middle of the riser at U=3.57 m/s and G_s=11.52 kg/m^2·s. It can be observed that pressure fluctuates in a fairly narrow band about zero.

Figure 2 shows the pressure fluctuations in the middle of the riser at U=3.57 m/s and G_s=19.24 kg/m^2·s. It is immediately evident that pressure fluctuates significantly more about zero for the higher G_s of 19.24 kg/m^2·s compared with the lower G_s of 11.52 kg/m^2·s depicted in Fig. 1. Specifically, the variability in the pressure fluctuations is significantly higher for G_s=19.24 kg/m^2·s compared with G_s=11.52 kg/m^2·s.

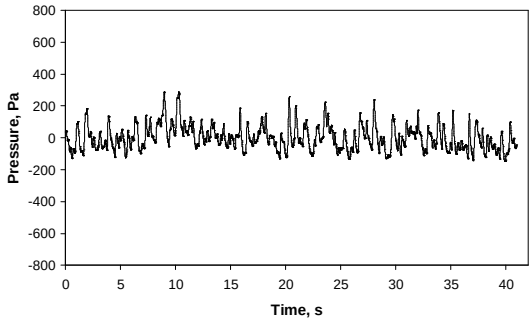

Fig. 1. Pressure fluctuations (normalized) in the middle of the riser at U=3.57 m/s and G_s=11.52 kg/m^2·s

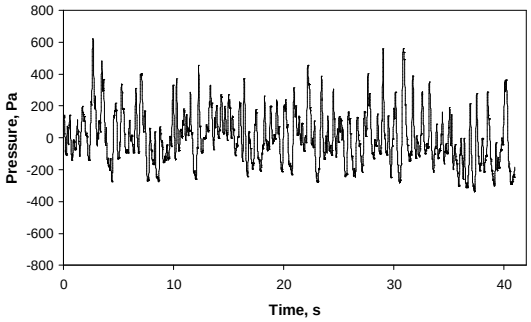

Fig. 2. Pressure fluctuations (normalized) in the middle of the riser at U=3.57 m/s and G_s=19.24 kg/m^2·s

However, the statement of “significantly higher” variability should be substantiated and statistically quantified. Therefore, statistical methods need to be applied to quantify the difference in variability. This becomes even more relevant when more than two reactor conditions are being evaluated at different values. In the study, three different superficial gas velocities and three different solids fluxes were evaluated for differences in pressure fluctuations along the riser.

STATISTICAL METHODOLOGY

The superficial gas velocity and solids flux are referred to as the reactor variables. Three values or conditions for each reactor variable were tested and the pressure fluctuations recorded. The pressure fluctuations will be evaluated in terms of its variability at the different reactor conditions (see Table 1). Note that pressure fluctuations were measured at three different positions in the fluidized bed i.e. at the bottom, middle and top of the riser.

The standard deviation has been used in a previous study by the authors for quantifying the variability of pressure fluctuations (7). In this paper, we introduce the Shannon entropy, H_X, and Fisher information matrix, I_X, as methods for evaluating the variability of pressure fluctuations.

Table 1. Experimental conditions

Condition	U, m/s	G_s, kg/m^2·s
1	3.57	11.52
2	3.57	14.78
3	3.57	19.24
4	4.17	17.79
5	4.17	21.75
6	4.17	26.76
7	4.78	29.65
8	4.78	34.17

The Shannon entropy is a well-known tool for investigating the degree of disorder in dynamical systems. The Shannon entropy will be high if the degree of disorder in the system is high. Let $\underline{x} = (x_1, x_2, \ldots, x_N)^T$ denote the sample of pressure fluctuations. The Shannon entropy (differential entropy) is given by the following formula (8):

$$H_X = -\int_{-\infty}^{\infty} f(x) \log f(x) dx \tag{1}$$

where $f(x)$ is the probability density function (PDF) of $\underline{x}$.

The Fisher information is a tool that can be used to accurately describe the behavior of dynamic systems and to characterize the complex signals generated by these systems (8). The Fisher information is defined as follows:

$$I_X = -\int_{-\infty}^{\infty} \left(\frac{\partial}{\partial x} f(x) \right)^2 \frac{dx}{f(x)} \tag{2}$$

In this paper we approximate the PDF with the kernel density estimation technique. Specifically, the PDF is approximated by:

$$\hat{f}_N(x, \lambda) = \frac{1}{\lambda N} \sum_{i=1}^{N} K\left(\frac{x - s_i}{\lambda} \right) \tag{3}$$

where s_i is the i-th pressure measurement, K is the kernel function and λ is the chosen bandwidth (14). A popular choice for the kernel is the Epanechnikov kernel given by:

$$K(u) = \begin{cases} \frac{3}{4}(1 - u^2) & if \quad u \in [-1,1] \\ 0 & if \quad u \notin [-1,1] \end{cases} \tag{4}$$

The kernel, $K(u)$, in eq. (4) is a continuous non-negative and symmetric function satisfying $\int_{-\infty}^{\infty} K(u) du = 1$. The bandwidth, λ, is estimated by minimizing the integrated mean squared error (IMSE):

$$IMSE(\lambda) = \int_{-\infty}^{\infty} \left(f(x) - \hat{f}_N(x, \lambda) \right)^2 dx \qquad (5)$$

Faraway and Jhun (14) proposed the estimation of the optimal λ with the bootstrap. As an example, Fig. 3 illustrates the estimation of the PDFs for the different conditions of U and G_s in Table 1 at the bottom of the reactor.

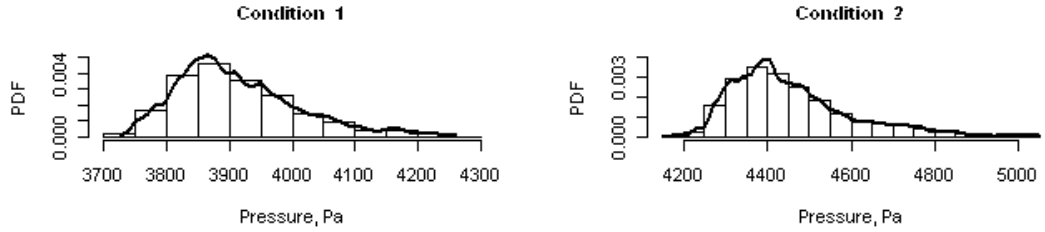

Fig. 3. PDF estimations for conditions 1 and 2 in Table 1 at the bottom of the reactor

STATISTICAL RESULTS

Figure 4 shows the relationship between the calculated Shannon entropy, H_X, and the U/G_s ratio for all conditions. The H_X increases with an increase in U and G_s. Several observations can be made from this figure; first, there is a significant drop in the entropy with an increase in the U/G_s ratio for all locations in the reactor. Second, there exists a significant difference between the entropy at the top of the reactor compared to that at the middle and bottom of the reactor. Therefore, there is significantly less variation or chaotic behavior of the fluidization process at the top of the reactor compared to the middle and bottom of the reactor.

Figure 5 shows the relationship between the I_X and the U/G_s ratio. Similar trends to the H_X are observed for the I_X; I_X decreases for an increase in the U/G_s ratio. Again, the I_X illustrates that there is significantly less variation at the top of the reactor compared to the middle and bottom of the reactor.

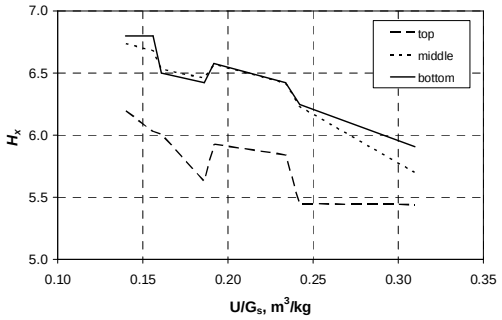

Fig. 4. Shannon entropy, H_X, as a function of U/G_s

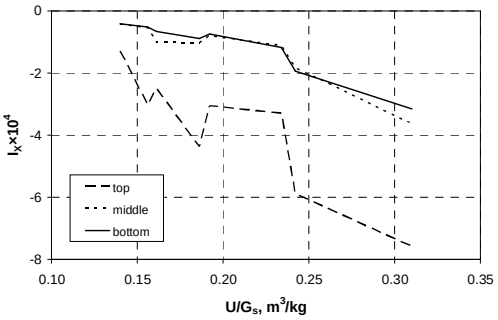

Fig. 5. Fischer information, I_X, as a function of U/G_s

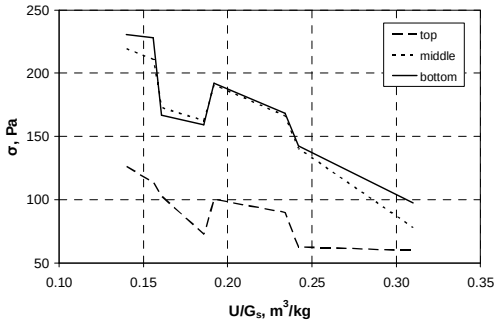

Fig. 6. Standard deviation, σ, as a function of U/G_s

Comparing with previous work (7), Fig. 6 shows the relationship between the standard deviation, σ, and U/G_s. Trends are similar to the H_X and the I_X; the σ decreases with an increase in U/G_s. Again, σ illustrates that there is significantly less variation in the fluidization process at the top of the reactor compared to the middle and bottom sections of the reactor.

The differences in the measures of variability, i.e. H_X, I_X, σ (also referred to as responses) between the locations in the reactor, as well as the relationship with U/G_s, can be quantified by constructing a statistical model to predict the measure of variability as a function of the location and U/G_s (15). Specifically, the linear model is of the form:

$$y_i = \tau_i z_i + \beta x \tag{6}$$

where y_i is the response variable for the *i-th* point or height in the reactor where the pressure measurements were made, i.e. top, middle or bottom, respectively; τ_i is the effect of the *i-th* location in the reactor on the response, and z_i is the dummy variable indicating the location in the reactor, i.e. $z_i = 1$ for the *i-th* location and zero otherwise. In Eq. (6) x is the U/G_s ratio, and τ_i (i=1, 2, 3) and β are parameters to be estimated from the least squares minimization.

Table 2. Parameters for linear models describing H_X, I_X and σ

Measure	**Location**	**Regression information**			
		Intercept, τ	Slope, β	Standard error	p-value
I_X	bottom	0.00032	-0.00216	0.00007	0.0001
	middle	0.00031			
	top	0.00005			
H_X	bottom	7.447	-4.873	0.13	0.0001
	middle	7.403			
	top	6.803			
σ	bottom	293.62	-594.74	20.05	0.0001
	middle	288.09			
	top	211.44			

Table 2 shows the results of fitting the Eq. (6) to the three measures of variability, H_X, I_X and σ. The standard error of the model, i.e. the square root of the sum of squares of errors divided by the number of observations minus 2, is very small for each model (note the standard error of the model is in the same units as the response). The p-value indicates the significance of the model, i.e. a p-value smaller than 0.05 indicates a 95%

confidence in the relationship between the variables and the measure of variability. Clearly, all three models in Table 2 are highly significant.

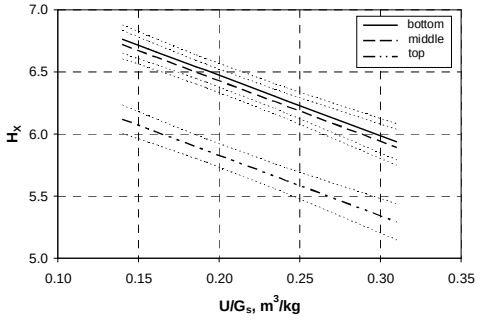

Fig. 7. Predicted entropy, H_X, as a function of U/G_s

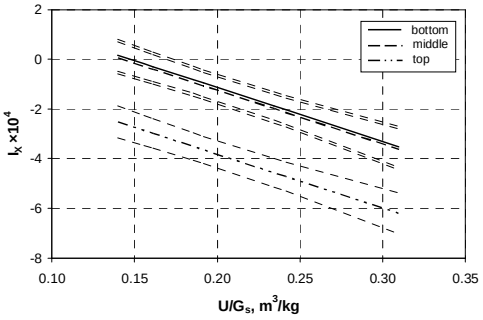

Fig. 8. Predicted Fischer information, I_X, as a function of U/G_s

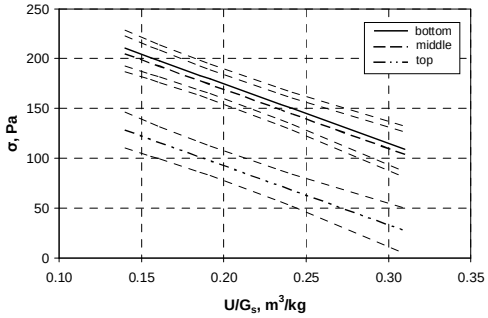

Fig. 9. Predicted standard deviation, σ, as a function of U/G_s

Equation (6), with the parameters in Table 2, can be used to predict the measures of variability for a given U/G_s and location in the reactor. As an illustration, Fig. 7 shows the predicted entropy, H_X, as a function of U/G_s and the location in the reactor. The 95% confidence bands are also indicated for each model. The 95% confidence band indicates the area about the regression model that captures the true relationship with 95% confidence. Note the significant difference between the relationship at the top of the reactor to the relationship at the bottom and middle of the reactor. Figures 8 and 9 show the predicted Fischer information, I_X, and the standard deviation, σ, respectively as a function of U/G_s and the location in the reactor. Similar trends to the entropy are observed.

CONCLUSIONS

The Shannon entropy analysis and Fisher information matrix analysis of pressure fluctuations are promising techniques to study the dynamics of gas-solid flow in fluidized beds. In this study, effects of two operating variables namely the superficial gas velocity, U, and solids circulation flux, G_s, on the Shannon entropy and Fisher information at different bed locations were determined. Both H_X and I_X follow the same trend; they decrease with increasing U/G_s. This result suggests that the fluidization process in CFBs with lower solids concentrations can be less chaotic than that in CFBs with high solids concentrations. The analysis also shows less variation at the top of the riser compared to its middle and bottom sections.

Simple linear statistical models have been developed to quantify the relationships between the measures of variability and U/G_s. The standard errors for these models are very small indicating that they are highly significant. The results confirm that both techniques can be use as tools to understand the complex dynamic behavior of gas-solid flows in CFBs.

ACKNOWLEDEMENT

Experimental data utilized in this paper were collected in the CFB cold model at Mintek.

NOTATION

G_s	– solids flux, kg/m^2·s	U	– gas velocity, m/s
H_X	– Shannon entropy	$\underline{x}$	– pressure vector
I_X	– Fisher information	β	– parameter in Eq. (6)
K(u)	– kernel function	λ	– band width
N	– number of pressure measurements	σ	– standard deviation

REFERENCES

1. M. Hartman, O. Trnka and K. Svoboda (2009). *Ind. Eng. Chem. Res*. **48**: 6830.
2. L. de Martin, J. Villa Briongos, J.M. Aragon and M.C. Palancar (2010). *Chem. Eng. Sci*. **65**: 4055.
3. A. Luckos and P. den Hoed (2004). *Ind. Eng. Chem. Res*. **43**: 5645.
4. A. Luckos and P. den Hoed (2005). In K. Cen (ed.) *Circulating Fluidized Bed Technology VIII*: 231–238. International Academic Publishers, Beijing.
5. A. Luckos and P. den Hoed (2005). In A. Luckos and P. Smit (eds.) *IFSA 2005, Industrial Fluidization South Africa:* 345–355. SAIMM, Johannesburg.
6. A. Luckos, Q.G. Reynolds and P. den Hoed (2007). In X. Bi, F. Berruti and T. Pugsley (eds) *Fluidization XII*: 145–152. ECI, New York.
7. R.L.J. Coetzer, A. Luckos and P. den Hoed (2008). In T. Hadley and P. Smit (eds.) *IFSA 2008, Industrial Fluidization South Africa*: 428-444. SAIMM, Johannesburg.
8. L. Telesca, R. Caggiano, V. Lapenna, M. Lovallo, S. Trippetta and M. Macchiato (2008). *Physica A* **1**: 6.
9. U. Lackermeier and J. Werther (2002). *Chem. Eng. Process*. **41**: 771.
10. C.M.H. Brereton and J.R. Grace (1993). In A.A. Avidan (ed.) *Circulating Fluidized Bed Technology IV:* 137–144. AIChE, New York.
11. Q.-Y. Zheng and H. Zhang (1995). In *Fluidization VIII, Preprint, Vol. 2:* 657–664. Progep, Toulouse, France.
12. T. Pugsley, D. LaPointe, B. Hirschberg and J. Werther (1997). *Can. J. Chem. Eng*. **75**: 1001.
13. Y. Jin, Z. Yu, C. Qi and D.-R. Bai (1988). In M. Kwauk and D. Kunii (eds.) *Fluidization' 88 Science and Technology:* 165–173. Science Press, Beijing.
14. J.J. Faraway and M. Jhun (1990). *J. American Statistical Association* **85**: 1119.
15. D.C. Montgomery (2001). *Design and analysis of experiments*. John Wiley & Sons, Inc.